International Journal of Technology

http://ijtech.eng.ui.ac.id

Research Article

Outage and Throughput Analysis of Cooperative Non-Orthogonal Multiple Access based SWIPT Cognitive Relay Network

Abdul Ali Khan[1,2], Punithavathi M. Thirunavakkarasu[1*], Nawaf Waqas[1]

[1]Communication Technology Section, Universiti Kuala Lumpur - British Malaysian Institute, Bt. 8, Jalan Sungai Pusu, 53100 Gombak, Selangor, Malaysia
[2]Faculty of Information & Communication Technology, Balachistan University of Information Technology, Engineering and Management Sciences, Quetta 87100, Pakistan
[*]Corresponding author: punitha@unikl.edu.my; Tel.: +03-61841000; Fax: +03-6186 4040

Abstract: This paper examines the performance of a half-duplex wireless sensor network (WSN) by using cooperative non-orthogonal multiple access (NOMA) integrated with simultaneous wireless information and power transfer (SWIPT) over Rayleigh fading channel to improve the performance of far and cognitive users in terms of spectrum efficiency, prolonging the coverage area, and network lifetime. Two distinct scenarios: one where a direct link exists between the source node S and the far user F, and another one where communication relies on an indirect path incorporating relay node N between node S and F. A new cooperative NOMA based SWIPT cognitive relay protocol is proposed, where a primary user S transmits a composite signal containing information of a near N and far user F, N which acts as an energy harvesting relay first apply NOMA to decode far user information to get its own information The remaining power is harvested by the relay node, and this harvested power is used to transmit information to both the far and cognitive users, respectively. The outage probabilities and throughputs are calculated. Simulated results show that the outage probability of far users with relay and direct link is reduced when compared with N after 25 dB SNR. This, in turn, improves the data rate of far/cell edge users.

Keywords: Cognitive radio; Cooperative NOMA; Outage probability; SWIPT

1. Introduction

Recently, the rapid expansion in the number of devices within the WSN has resulted in substantial connectivity and a heightened demand for spectrum and power usage (Kurniawati et al., 2023; Hendrarini et al., 2022). Enhanced spectral efficiency, prolonging the coverage area, and network lifetime are major concerns in the area of WSN (Priyadarshi & Gupta, 2020; Yetgin et al., 2017; Jorswieck et al., 2014).

Enhancing the spectral efficiency of a WSN through NOMA has received considerable importance (Abuajwa & Mitani, 2024; Khan et al., 2020; Sedtheetorn & Chulajata, 2016). Unlike, conventional multiple access (MA) schemes (Ramly et al., 2023; Adriansyah et al., 2015; Sun et al.,

This work was supported by the Malaysian Ministry of Higher Education through the Fundamental Research Grant Scheme (FRGS/1/2021/TK0/UNIKL/02/3).

https://doi.org/10.14716/ijtech.v16i1.7209
Received July 2024; Revised August 2024; Accepted October 2024; Published January 2025

2015), NOMA differentiates users in the power domain rather than frequency, time, and code division MA (Ding et al., 2016). At the base station, the simultaneous sharing of resources is achieved by utilizing power-domain multiplexing, also known as power-domain superposition coding (SC) (Su et al., 2016a).

In NOMA, more power is allocated to users with poor channel conditions, while less power is assigned to users with better channel conditions. At the receiving end, users can decode the desired information using successive interference cancellation (SIC) techniques (Haci, 2018; Ali et al., 2016; Su et al., 2016b). Moreover, NOMA can support a significantly larger number of users compared to OMA through the utilization of non-orthogonal resource allocation, which meets the rapidly growing demand for user access needed for the Internet of Things in future WSN (Dai et al., 2018; Hojeij et al., 2015).

In addition to spectral efficiency, another key objective is to reduce the probability of outage events for cell edge users, which results in improved WSN performance. The challenge of providing reliable service to cell-edge users from the base station is well-documented, primarily due to the inherent weakening of signal strength over distance and interference from other base stations (Mukherjee et al., 2021; Park et al., 2016; Tseng et al., 2012). As reported in (Shin et al, 2017) NOMA can improve the channel conditions of cell-edge users. However, it still has limitations that prevent cell-edge users from achieving the same throughput as users closer to the base station. Achieving equitable data rates between cell-center and cell-edge users requires a significant reduction in the power allocated to users closer to the cell center (Huang & Zhou, 2021; Vinh et al., 2019). Cooperative NOMA played a part in reducing the probability of outage events for cell edge users and improve throughput, by successfully decoding the information of the far users at the near users having good channel conditions. These users will act as relays to provide strong channel conditions to the far users who have worse channel conditions from the base station (Elsaraf et al., 2021; Yang et al., 2017).

To elevate network performance to the next level by prolonging the lifetime of a WSN, radio frequency (RF) based wireless power transfer (WPT) is used to increase the lifetime of energy-constrained wireless sensor nodes in the network. An emerging solution is to scavenge energy from the ambient RF signals present in the environment (Varshney, 2008). The major advantage of this solution is that the RF signal can carry both (information and energy) at the same time. Thus, the idea of SWIPT was proposed that the energy-limited sensor nodes at the receiving end with the capacity for simultaneous information decoding and energy harvesting, the receiving nodes utilize the RF signal for dual purposes, which does not hold in practice (Zuhra et al., 2022) (Fouladgar & Simeone, 2012) (Popovski et al., 2012). To address this limitation, a practical receiver design with dedicated components for information decoding and energy harvesting has become widely accepted in the recent literature (Arakawa et al., 2024; Clerckx et al., 2022; Clerckx et al., 2019). Recent research has predominantly focused on (point-to-point) communication systems with SWIPT, building upon the extensive work already present in the. The integration of SWIPT into wireless cooperative sensor networks and two popular cooperative relaying networks (amplify and forward) and (decode and forward) has been a prominent theme in recent research. In addition to this, for (amplify and forward) relaying, time switching (TS) and power splitting (PS) based relaying protocols were proposed by (Nasir et al., 2013). In contrast, authors (Liu et al., 2016) proposed a new antenna switching protocol for (decode and forward) relaying to lower its complexity. To enhance both spectral and power efficiency, the concept of a SWIPT-based cognitive relay network was proposed by (Gurjar et al., 2020). In (Zhou et al., 2021) authors presented a GS-Dinkel Bach algorithm aimed at improving energy efficiency in NOMA-SWIPT cooperative relay networks. The proposed algorithm leads to substantial gains in both direct-link and cooperative transmission modes while also decreasing the computational overhead. Authors (Ahlgren et al., 2022) centre their attention on conducting an in-depth analysis of system performance metrics, including outage probability, throughput, and energy efficiency, specifically within the context of IoT networks that operate under the conditions of Nakagami-m fading. In (Li et al., 2023), introduced two innovative SWIPT-

based cooperative protocols, namely SWIPT-CNOMA-PS and SWIPT-CNOMA-TS. These protocols are specifically engineered to elevate the quality of communication experienced by users situated at the edge of the cell coverage area. In (Baranwal et al., 2024), the authors explore a full-duplex cooperative NOMA system that utilizes SWIPT to provide service to both distant and nearby IoT users.

While previous studies contribute significantly to the field, they exhibit certain limitations when compared to the comprehensive scope of this work. Many focus narrowly on optimizing energy efficiency without conducting a complete performance evaluation that includes key metrics such as outage probability and throughput. Furthermore, several approaches propose basic cooperative protocols but do not integrate cognitive relay strategies or adaptive power allocation mechanisms, which are both critical for optimizing overall system performance. Full-duplex systems, though explored, often struggle with self-interference, a challenge that this research addresses through the implementation of cognitive relay systems, ensuring enhanced reliability, spectral efficiency, and overall network performance.

This paper presents a new cooperative NOMA-based SWIPT cognitive relay protocol by introducing cooperative NOMA in SWIPT-based cognitive relay networks. Where a primary user transmits a composite signal containing information of a near and far user, the near user, which acts as an energy harvesting relay first applies NOMA to decode far user information to get its own information. The remaining power is utilized by the relay node for energy harvesting, and the harvested power is then used to transmit information to far and cognitive users, respectively. This, in turn, improves power efficiency, spectral efficiency, and the coverage range of the WSN. Additionally, the outage probabilities and throughputs are calculated for half-duplex without direct link and half-duplex with direct link.

2. System model hods

Our considered system model comprises a source node (S), a near-user node (N), a far-user node (F), and a cognitive node (C). In this model, the near user (N) is an intermediate energy-limited relay node to assist the S-to-F data transmission. The process begins with the relay node (N) applying Non-Orthogonal Multiple Access (NOMA) to decode the information intended for the far user (F). This integration of NOMA allows multiple users (N and F) to share the same frequency spectrum by assigning different power levels, significantly enhancing spectral efficiency by allowing simultaneous data transmission within the same bandwidth.

Once the far user's signal is successfully decoded, the near user (N) employs the Power-Splitting Relaying (PSR) protocol to simultaneously decode its own signal and harvest energy from the incoming transmission. This ensures that the relay node utilizes only the minimum necessary energy for decoding while efficiently harvesting the remaining energy. This dual functionality significantly improves power efficiency, as the harvested energy can be reused for multiple transmissions, eliminating the need for additional external power sources.

The harvested energy is then split between forwarding the far user’s information signal and relaying its own sensed data to the cognitive user (C). This process enables N to opportunistically reuse radio resources, thereby performing simultaneous N-to-F and N-to-C communications. Such opportunistic spectrum reuse maximizes available bandwidth utilization, further enhancing spectral efficiency. Moreover, this approach extends the coverage range, as the near user (N) acts as a cooperative relay, assisting the far user (F) in overcoming transmission limitations and effectively extending the communication range of the network.

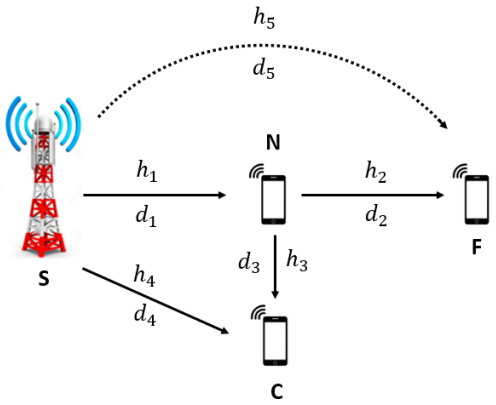

Figure 1 A schematic representation of the system model

The system model under consideration is illustrated in Figure 1, where 'd' and 'h'(I,j ∈ {S, N, C, F}) represent the distance and channel coefficients between the nodes, respectively. All the channel gains between the WSN nodes are modeled as quasi-static Rayleigh fading channels; for each transmission block, channel coefficients are constant but vary independently between different transmission blocks. A distance-dependent path loss model has been modeled between the communicating nodes with a rate d^{-a}, where d is the distance between nodes and a is the path loss exponent.

Furthermore, in this paper, we have considered two different cases.

Case I: When a direct communication link exists for transmitting information between nodes (S and F) in addition to the relay node link.

Case II: When a relay node is required for communication between nodes (S and F) and has no direct link.

2.1. Cooperative NOMA, Energy harvesting, and Cognitive Radio operations

As illustrated in Figure 1, the overall communication process consists of two phases. In phase one, source node S transmits a signal containing information of a near and far user $z_1x_1 + z_2x_2$ during time slot W_1. Where z_1 and z_2 are the power allocation coefficients and x_1 and $x_2$are the information of far node F and near node N, respectively. The signal observed at N and C is given by Equation 1 and Equation 2:

$$Y_{\mathrm{N}} = \sqrt{P_{\mathrm{S}}} \sum_{k\in\{1,2\}} z_k x_k \frac{h_1}{\sqrt{1+d_1^{\alpha}}} + \eta_1 \quad (1)$$

$$Y_{\mathrm{C}} = \sqrt{P_{\mathrm{S}}} \sum_{k\in\{1,2\}} z_k x_k \frac{h_4}{\sqrt{1+d_4^{\alpha}}} + \eta_4 \quad (2)$$

Where Y_{N} represent the signal observed at N, P_S is the transmit power from the source node S, h_1 is the small-scale Rayleigh fading from S to R, η_1 is the additive white gaussian noise (AWGN) at N having a variance σ^2, d_1 is the distance between S and N, and a represents the path loss exponent in Equation 1. In Equation 2, Y_{N} represent the signal observed at C, P_S is the transmit power from the source node S, h_4 is the small-scale Rayleigh fading from S to C, η_4 is the additive white gaussian noise (AWGN) at C having a variance σ^2, d_4 is the distance between S and C, and a represents the path loss exponent

For NOMA to be effective $|z_1| > |z_2|$ with $|z_1| + |z_2| = 1$. To detect x_1, the received signal to noise ratio (SINR) at N is given by Equation 3:

$$\gamma_{\mathrm{F-N}} = \frac{\rho|h_1|^2|z_1|^2}{\rho|h_1|^2|z_2|^2+1+d_1^{\alpha}} \quad (3)$$

Where $\gamma_{\mathrm{F-N}}$ represents the SINR of F at N, ρ represents the transmit signal-to-noise ratio (SNR) (assuming $\sigma^2 n = \sigma^2 f = \sigma^2$). It is assumed that the near node is equipped with a rechargeable battery and the ability to split received power for SWIPT. The signal observed at relay node N is divided into two parts. A portion of the energy is dedicated to decoding information, while the rest

is harvested to support the transmission of node S information to F and its own information to node C (see Equation 4). Thus,

$$Y_{\mathrm{N}} = \sqrt{P_{\mathrm{S}}} \sum_{k\in\{1,2\}} z_k x_k \frac{\sqrt{1-\beta} h_1}{\sqrt{1+d_1^{\alpha}}} + \eta_1 \quad (4)$$

Where β represents the power splitting coefficient, which dictates the portion of received signal energy allocated for harvesting (Varshney, 2008), h_1 represents the channel coefficient from S to N, η_1 is AWGN at node N, with variance $\sigma^2 n$ and d_1 is the distance between node S and N.

Node N employs a SIC technique to decode both its own information and that of node F. More specifically, N initially decodes F's message and then extracts its information by subtracting this decoded message from its received signal. Thus, SINR at N for detecting the message x_1 of F can be expressed as (see Equation 5):

$$\gamma_{\mathrm{F-N}} = \frac{\rho|h_1|^2|z_1|^2(1-\beta)}{\rho|h_1|^2|z_2|^2(1-\beta)+1+d_1^{\alpha}} \quad (5)$$

The received SNR of N to detect x_2 of a near node N is given by (see Equation 6):

$$\gamma_{\mathrm{N-N}} = \frac{\rho|h_1|^2|z_2|^2(1-\beta)}{1+d_1^{\alpha}} \quad (6)$$

The amount of harvested energy determined by N solely depends upon the power splitting coefficient β. Based on Equation 5, the data rate supported by medium from S to N for decoding the F message x_1 is given by

$$R_{x_1} = \frac{1}{2}\log\left(1 + \frac{\rho|h_1|^2|z_1|^2(1-\beta)}{\rho|h_1|^2|z_2|^2(1-\beta)+1+d_1^{\alpha}}\right) \quad (7)$$

For our analysis, we assumed that the energy consumed in receiving and processing information is considered negligible relative to the energy required for transmission. In this scheme, dynamic PSR protocol is applied. This implies that β is not a constant value; rather, it is a variable dynamically tuned to maximize the assistance provided to node N during transmission

Our target is to first ensure the detection of far NOMA user F message at near NOMA user N and the detection of near NOMA user N message at N. Then the remaining energy is harvested by N. In this case, based on Equation 7, to guarantee that N can successfully decode the message of F, we have a rate $R_1 = R_{x_1}$. Therefore, the β is set as follows

$$\beta = max\left\{0{,}1 - \frac{\tau 1(1+d_1^{\alpha})}{P_s h_1 z_2}\right\} \quad (8)$$

Where the threshold of F ($\tau 1 = 2^{2R_1} - 1$), here $\beta = 0$ signifies that all the energy is used by N for information decoding, with no energy left for harvesting. The energy harvested at N is given by

$$E_{\mathrm{N}} = \frac{WnP_s\beta_i|h_1|^2}{2(1+d_1^{\alpha})} \quad (9)$$

Where W represents the entire duration of the transmission process, encompassing both the source-to-destination transmission and the relay-aided transmission and n represents the energy harvesting coefficient. The transmit power at N can be expressed as:

$$P_{\mathrm{N}} = \frac{n\beta_i|h_1|^2}{1+d_1^{\alpha}} \quad (10)$$

In phase two, by utilizing the harvested energy, node N forwards the combined far user information signal and its sensed information to nodes F and C, respectively. Note that here, N reuses both the radio and power resources of the primary network. Therefore, the received signal at nodes F and C can respectively be expressed as:

$$Y_{\mathrm{N-F}} = \sqrt{\frac{P_{\mathrm{N}}}{d_2^{\alpha}}} h_2 x_1(L) + \sqrt{\frac{P_{\mathrm{N}}}{d_2^{\alpha}}} h_2 x_n(1-L) + \eta_2 \quad (11)$$

$$Y_{\mathrm{N-C}} = \sqrt{\frac{P_{\mathrm{N}}}{d_3^{\alpha}}} h_3 x_{\mathrm{n}}(1-L) + \sqrt{\frac{P_{\mathrm{N}}}{d_3^{\alpha}}} h_3 x_1(L) + \eta_3 \quad (12)$$

Where $Y_{\mathrm{N-F}}$ Equation 11 represents near user N signal (containing F and C user information) at F and $Y_{\mathrm{N-C}}$ in Equation 12 represents near user N signal (containing F and C user information) at C, x_n represent the information of near for C user, and L represents the power allocation coefficient for the F user.

Based on Equation 11 and Equation 12, the received SINR at nodes F and C can respectively be written as

$$\gamma_{\mathrm{F-F}} = \frac{P_{\mathrm{N}}|h_2|L}{P_{\mathrm{N}}|h_2|(1-L)+1+d_2^{\alpha}} \tag{13}$$

$$\gamma_{\mathrm{C-C}} = \frac{P_{\mathrm{N}}|h_3|(1-L)}{P_{\mathrm{N}}|h_3|L+1+d_3^{\alpha}} \tag{14}$$

Since node C has already received the message of F in phase I (see Equation 2), the interference cancellation technique is applied to get the desired message of node C. Based on this, we can rewrite the SNR of node C.

$$\gamma_{\mathrm{C-C}} = \frac{P_{\mathrm{N}}|h_3|(1-L)}{1+d_3^{\alpha}} \tag{15}$$

Case I: Direct Link

Case ll: Without a direct link

2.2. Outage probability and throughput analysis

The sensor node experiences an outage if the received (SNR/SINR) falls below a predefined threshold. The probability of outage events occurring in the primary communication links (S to N, N to F, and S to F) under Case I conditions can be calculated as:

$$P_{\mathrm{out}}^{\mathrm{F-N}} = P_{\mathrm{r}}(\gamma_{\mathrm{F}} < th_{-f}) + P_{\mathrm{r}}(\gamma_{\mathrm{F-N}} < th_{-f}, \gamma_{\mathrm{N-N}} < th_{-n}) \tag{16}$$

$$Q_1 = P_{\mathrm{r}}(\gamma_{\mathrm{F}} < th_{-f})$$

$$Q_2 = P_{\mathrm{r}}(\gamma_{\mathrm{F-N}} < th_{-f}, \gamma_{\mathrm{N-N}} < th_{-n})$$

Where th_{-f} and th_{-n} represents the threshold of F and N users and the terms Q_1 and Q_2 in Equation 16 indicate that an outage event in the primary communication link (S to N) occurs when the received SNR/SINR at N for both N and F is below the decoding threshold.

$$P_{\mathrm{out(dl)}}^{\mathrm{F-F}} = P_{\mathrm{r}}(\gamma_{\mathrm{MRC}} < th_{-f}, \gamma_{\mathrm{F-N}} \geq th_{-f}) + P_{\mathrm{r}}(\gamma_{\mathrm{F\_F}} < th_{-f}, \gamma_{\mathrm{F-N}} < th_{-f}) \tag{17}$$

$$U_1 = P_{\mathrm{r}}(\gamma_{\mathrm{MRC}} < th_{-f}, \gamma_{\mathrm{F-N}} \geq th_{-f})$$

$$U_2 = P_{\mathrm{r}}(\gamma_{\mathrm{F\_F}} < th_{-f}, \gamma_{\mathrm{F-N}} < th_{-f})$$

Here γ_{MRC} represents ($\gamma_{\mathrm{MRC}} = SINR\ of\ F\ direct\ link\ at\ F + SINR\ of\ F\ through\ N\ at\ F$) and the terms U_1 and U_2 in (equations 17) shows that the probability of outage events occurring in the primary communication link (S to N and N to F) and (S to F) direct link occurs when the received SNR/SINR of F at F, F at N, and γ_{MRC} of F at F is less than the decoding threshold.

$$P_{\mathrm{out}}^{\mathrm{F-F}} = P_{\mathrm{r}}(\gamma_{\mathrm{F}} < th_{-f}, \gamma_{\mathrm{F-N}} \geq th_{-f}) + P_{\mathrm{r}}(\gamma_{\mathrm{F\_F}} < th_{-f}, \gamma_{\mathrm{F-N}} < th_{-f}) \tag{18}$$

$$V_1 = P_{\mathrm{r}}(\gamma_{\mathrm{F}} < th_{-f}, \gamma_{\mathrm{F-N}} \geq th_{-f})$$

$$V_2 = P_{\mathrm{r}}(\gamma_{\mathrm{F\_F}} < th_{-f}, \gamma_{\mathrm{F-N}} < th_{-f})$$

The terms $V_1$and V_2in Equation 18 shows that the probability of outage events occurring in primary communication links without direct link case II (S to N to F) occurs when the received SNR/SINR of F at F and F at N is less than the decoding threshold.

$$P_{\mathrm{out}}^{\mathrm{CU}} = P_{\mathrm{r}}(\gamma_{\mathrm{C-C}} < th_{-c}) \tag{19}$$

In Equation 19, the probability of outage events of the secondary communication link (N to C) occurs when the received SNR/SINR of C at C is less than the decoding threshold.

Based on $P_{\mathrm{out}}^{\mathrm{F-N}}$ and $P_{\mathrm{out}}^{\mathrm{F-F}}$in Equations 16 and 17, the achievable throughput of the primary communication link (S to N) and (S to N and N to F) with (S to F) direct link case I is given by

$$C_{\mathrm{N}} = \left(1 - P_{\mathrm{out}}^{\mathrm{F-N}}\right) R_1 (W/2)/W \tag{20}$$

$$C_{\mathrm{F}} = \left(1 - P_{\mathrm{out(dl)}}^{\mathrm{F-F}}\right) R_2 (W/2)/W \tag{21}$$

Where W/2 indicates the actual time available for successful transmission.

Based on $P_{\mathrm{out}}^{\mathrm{F-F}}$ the achievable throughput of the primary communication link (S to N and N to F) case I is given by

$$C_{\mathrm{F}} = \left(1 - P_{\mathrm{out}}^{\mathrm{F-F}}\right) R_2 (W/2)/W \tag{22}$$

Based on $P_{\text{out}}^{\text{CU}}$ the achievable throughput of the secondary communication link (N to C) is given by

$$C_{\text{C}} = \left(1 - P_{\text{out}}^{\text{CU}}\right) R_2 (W/2)/W \tag{23}$$

3. Performance evaluation

In this section, simulation results are presented to provide a detailed understanding of the WSN. The impact of varying system parameters on network performance is assessed. Unless otherwise stated, we set the energy conversion efficiency $n = 0.8$, and power allocation coefficients are (z_1= 0.60 for far user F) and ($z_2 = 0.40$ for near user N). The distance between the source-to-near node is set to 4 m, the near-to-far node is set to 2 m, and the near-to-cognitive node is set to 2 m. The transmission rates for near, far, and cognitive users are (R_1= 0.5, R_2= 0.5, and R_3= 0.3) bits/s/Hz, respectively.

The outage probability and achievable throughput of near (N), far (F), cognitive (C), and far with direct link, with varying transmit SNR, are shown in Figures 2(a) and 2(b), respectively. It's shown in Figure 2(a) that the outage probability at N, F, and C nodes decreases as the value of transmitting SNR increases. As the value of SNR increases, the received SINR at destination nodes increases, which as result decreases the outage probability at destination nodes [see equation (16, 17, 18, and 19)]. More specifically, in Figure 2(a), as the transmit SNR increases from 25 dB onwards, the outage probability of far node F with direct link starts reducing as compared to near node N. At low transmit SNR, the effect of the direct link on the maximum ratio combining MRC is not significant due to the large distance between node S to F, which results in high path loss and greater outage probability. This indicates that the direct link becomes more beneficial at higher SNR values, improving the far user's reliability.

In addition to this, as shown in Figure 2(b), achievable throughput at destination nodes S, F, and C increases as the SNR increases. As the outage probability depends upon the transmit SNR, outage probability decreases as transmit SNR increases because it results in higher SINR at the receiving nodes. Consequently, the system's overall throughput improves, demonstrating that the proposed protocol effectively utilizes available energy and spectrum resources, enhancing communication performance in wireless sensor networks.

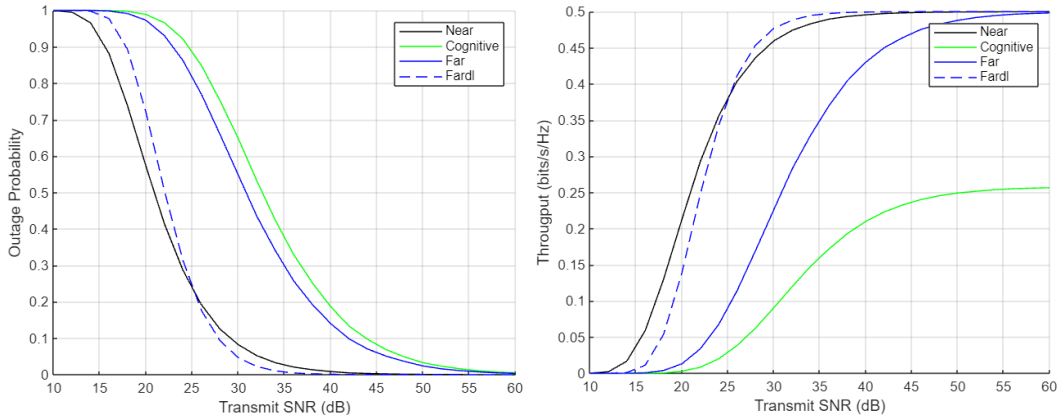

Figure 2 Transmit SNR with $a = 2$, and R_1= 0.5, R_2= 0.5 and R_3= 0.3 bits/s/Hz versus (a) Outage probability (b) Throughput

Figure 3(a) and 3(b) illustrate the impact of increasing the far user's rate from 0.5 to 0.55- and 0.60-bits/s/Hz on the outage probability of both the near user (N) and the far user (F). A higher data rate for the far user leads to a greater frequency of outages for both the far user and the far user with a direct link. Furthermore, it can be seen that the outage probability for the near user rises as the data rate (R_1) of the far user increases. This is due to the design of our proposed protocol, where the near user N must first decode the message intended for the far user F (x_1) before decoding its

message (x_2). Therefore, increasing (R_1) makes decoding (x_1) more challenging, resulting in a higher outage rate. A critical observation is that the outage probability will always be one if (R_1) and (R_2) are not chosen correctly. Specifically, for the selection of R_1 it should satisfy the condition ($|z_1|^2 - |z_2|^2\tau_1 > 0$) to guarantee the successful implementation of SIC. The choice of R2 should ensure that the energy split required to detect (x_1) is also sufficient to detect (x_2). This emphasizes the importance of selecting optimal power allocation coefficients to maintain reliable communication. If these parameters are not carefully adjusted, it could lead to system inefficiencies and significantly degrade the overall network performance.

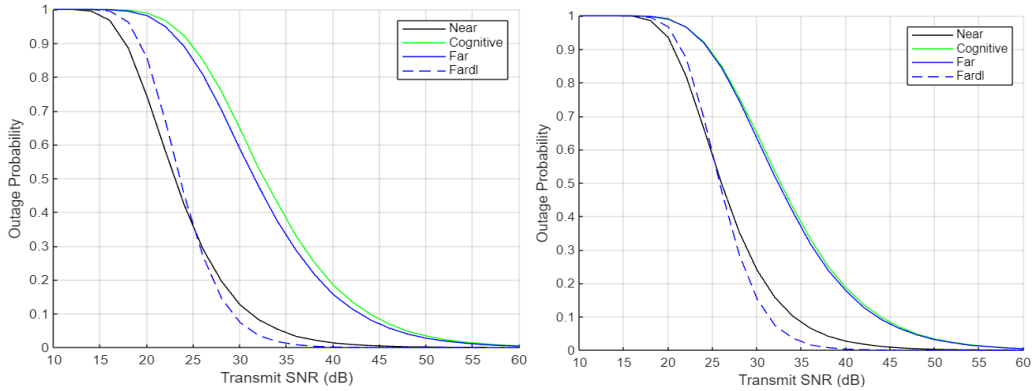

Figure 3 Outage probability of the near, far, and cognitive users versus SNR with $a = 2$, R_2= 0.5 and R_3= 0.3 bits/s/Hz (a) R_1= 0.55 bits/s/Hz and (b) R_1= 0.60 bits/s/Hz

The outage probability of near, far, and cognitive users was evaluated by changing the path loss exponent coefficient from α = 2, to 3 and 4. The path loss exponent values (α = 2, 3, and 4) were selected in our simulations based on their relevance to practical wireless communication environments. Specifically, α=2 represents an ideal free-space propagation scenario with minimal obstacles, while α = 3 and α = 4 correspond to more realistic environments with moderate to high signal attenuation due to obstacles, such as urban or indoor settings. Figures 4a and 4b visually represent the relationship between outage probability, SNR, and path loss coefficients for near, far, and cognitive users. It can be seen in Figure 2 that the outage probability of near, far, and cognitive is low when the path loss exponent is α = 2. By changing the path loss exponent to 3 and 4 we can see that the outage probability increases with the increase in path loss exponent coefficient. This shows that the proposed protocol has low outage and high throughput for path loss exponent coefficient 2.

As the path loss exponent increases, signal degradation becomes more pronounced, which highlights the importance of deploying this protocol in scenarios with favourable propagation conditions for optimal performance.

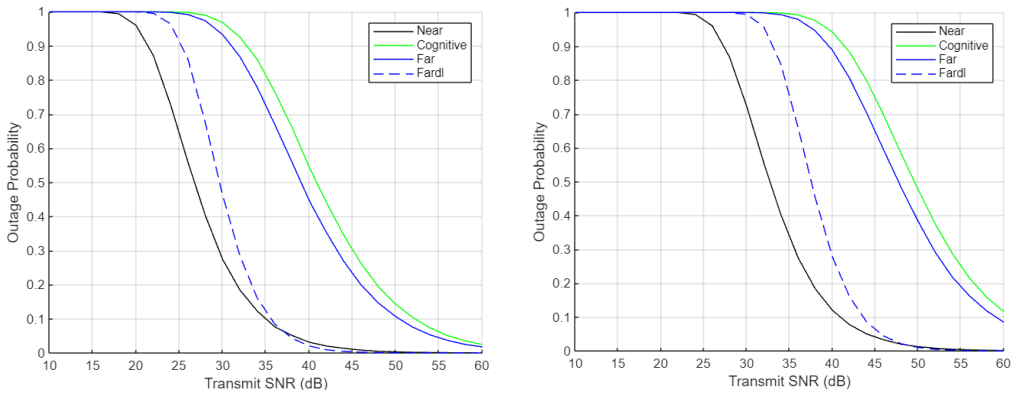

Figure 4 Outage probability of the near, far, and cognitive users versus SNR having R_1= 0.5, R_2= 0.5 and R_3= 0.3 bits/s/Hz (a) $a = 3$ and (b) $a = 4$

4. Conclusions

This paper presents a novel cooperative NOMA-based SWIPT cognitive relay protocol for WSNs. By using cooperative NOMA for efficient resource allocation and SWIPT for energy harvesting at the relay node, we aimed to improve overall network performance. The protocol uses the relaying energy limit node to enhance the power efficiency, spectral efficiency, and coverage range of the WSN by successfully sending far and cognitive user information. The simulation result demonstrated the protocol's ability to improve reliability (lower outage) and data rates (higher throughput) for (near and far) users as the relay node has no power. Notably, the far user with the direct link has low outage and high data rate as compared to the near user as the SNR increases from 25 dB. Moreover, simulation results show the impact of far user data rate revealed a trade-off between improving far user performance and maintaining reliable communication for the near user. This underscores the importance of careful parameter tuning to optimize the system's overall performance. Finally, our analysis of the path loss exponent highlighted the protocol's sensitivity to signal attenuation. The results indicate that the protocol is most effective in environments with lower path loss, such as those characterized by a path loss exponent of 2. In conclusion, this research establishes the potential of the proposed protocol to enhance the performance of WSNs, especially in scenarios with moderate path loss. For future work investigation of adaptive power allocation strategies to dynamically adjust to varying channel conditions using machine learning techniques.

Acknowledgements

This work was supported by the Malaysian Ministry of Higher Education (MOHE) through the Fundamental Research Grant Scheme (FRGS/1/2021/TK0/UNIKL/02/3).

Author Contributions

Abdul Ali Khan and Nawaf Waqaf developed the model and performed the simulations, analysed the data and wrote the manuscript. Punithavathi Thirunavakkarasu contributed to the analysis and final version of the manuscript and supervised the project.

Conflict of Interest

The authors declare that they have no known competing financial interests or personal relationships that could have appeared to influence the work reported in this paper.

References

Abuajwa, O & Mitani, S 2024, 'Dynamic resource allocation for energy-efficient downlink NOMA systems in 5G networks', Heliyon, vol. 10, no. 9, https://doi.org/10.1016/j.heliyon.2024.e29956

Adriansyah, N, Asvial, M, & Budiarjo, B 2015, 'Exploiting geometrical node location for improving spatial reuse in SINR-based STDMA multi-hop link scheduling algorithm', *International Journal of Technology*, vol. 6, no. 1, pp. 53-62, https://doi.org/10.14716/IJTECH.V6I1.781

Ahlgren, F, Maleki, N, Zapico, JL, Nguyen, TT, Nguyen, SQ, Nguyen, PX, & Kim, YH 2022, 'Evaluation of full-duplex SWIPT cooperative NOMA-based IoT relay networks over Nakagami-m fading channels', *Sensors*, vol. 22, no. 5, pp. 1974, https://doi.org/10.3390/S22051974

Ali, MS, Tabassum, H, & Hossain, E 2016, 'Dynamic user clustering and power allocation for uplink and downlink non-orthogonal multiple access (NOMA) systems', *IEEE Access*, vol. 4, pp. 6325-6343, https://doi.org/10.1109/ACCESS.2016.2604821

Arakawa, T, Krogmeier, JV, & Love, DJ 2024, 'Theoretical and practical analysis of MIMO simultaneous wireless information and power transfer over inductively coupled circuits', *IEEE Transactions on Antennas and Propagation*, vol. 72, no. 3, pp. 2780-2789, https://doi.org/10.1109/TAP.2022.3218926

Baranwal, A, Sharma, S, Roy, SD, & Kundu, S 2024, 'On performance of a full duplex SWIPT enabled cooperative NOMA network', *Wireless Networks*, vol. 30, no. 3, pp. 1643-1656, https://doi.org/10.1007/S11276-023-03608-X

Clerckx, B, Kim, J, Choi, KW, & Kim, DI 2022, 'Foundations of wireless information and power transfer: theory, prototypes, and experiments', *Proceedings of the IEEE*, vol. 110, no. 1, pp. 8-30, https://doi.org/10.1109/JPROC.2021.3132369

Clerckx, B, Zhang, R, Schober, R, Ng, DWK, Kim, DI, & Poor, HV 2019, 'Fundamentals of wireless information and power transfer: from RF energy harvester models to signal and system designs', *IEEE Journal on Selected Areas in Communications*, vol. 37, no. 1, pp. 4-33, https://doi.org/10.1109/JSAC.2018.2872615

Dai, L, Wang, B, Ding, Z, Wang, Z, Chen, S, & Hanzo, L 2018, 'A survey of non-orthogonal multiple access for 5G', *IEEE Communications Surveys and Tutorials*, vol. 20, no. 3, pp. 2294-2323, https://doi.org/10.1109/COMST.2018.2835558

Ding, Z, Fan, P, & Poor, HV 2016, 'Impact of user pairing on 5G nonorthogonal multiple-access downlink transmissions', *IEEE Transactions on Vehicular Technology*, vol. 65, no. 8, pp. 6010-6023, https://doi.org/10.1109/TVT.2015.2480766

Vinh, HD, Son, VV, Hoang, TM, & Hiep, PT 2019, 'Proposal of combination of NOMA and beamforming methods for downlink multi-users systems', *In;* 3rd International Conference on Recent Advances in Signal Processing, Telecommunications & Computing (SigTelCom)

Elsaraf, Z, Ahmed, A, Khan, FA, & Ahmed, QZ 2021, 'Cooperative non-orthogonal multiple access for wireless communication networks by exploiting the EXIT chart analysis', *Eurasip Journal on Wireless Communications and Networking*, vol. 2021, no. 1, pp. 1-14, https://doi.org/10.1186/S13638-021-01961-Z

Fouladgar, AM, & Simeone, O 2012, 'On the transfer of information and energy in multi-user systems', *IEEE Communications Letters*, vol. 16, no. 11, pp. 1733-1736, https://doi.org/10.1109/LCOMM.2012.091212.121660

Gurjar, DS, Nguyen, HH, & Tuan, HD 2020, 'Wireless information and power transfer for IoT applications in overlay cognitive radio networks', *IEEE Internet of Things Journal*, vol. 6, no. 2, pp. 3257 - 3270, https://doi.org/10.1109/JIOT.2018.2882207

Haci, H 2018, 'Performance study of non-orthogonal multiple access (NOMA) with triangular successive interference cancellation', *Wireless Networks*, vol. 24, no. 6, pp. 2145-2163, https://doi.org/10.1007/S11276-017-1464-7

Hendrarini, N, Asvial, M, & Sari, RF 2022, 'Wireless sensor networks optimization with localization-based clustering using game theory algorithm', *International Journal of Technology*, vol. 13, no. 1, pp. 213-224, https://doi.org/10.14716/IJTECH.V13I1.4850

Hojeij, MR, Farah, J, Nour, CA, & Douillard, C 2015, 'Resource allocation in downlink non-orthogonal multiple access (NOMA) for future radio access', *IEEE Vehicular Technology Conference*, 2015, https://doi.org/10.1109/VTCSPRING.2015.7146056

Huang, Y, & Zhou, L 2021, 'MISO NOMA downlink beamforming optimization with per-antenna power constraints', *Signal Processing*, vol. 179, article 107828, https://doi.org/10.1016/J.SIGPRO.2020.107828

Jorswieck, E, Badia, L, Fahldieck, T, Karipidis, E, & Luo, J 2014, 'Spectrum sharing improves the network efficiency for cellular operators', *IEEE Communications Magazine*, vol. 52, no. 3, pp. 129-136, https://doi.org/10.1109/MCOM.2014.6766097

Khan, WU, Liu, J, Jameel, F, Sharma, V, Jantti, R, & Han, Z 2020, 'Spectral efficiency optimization for next generation NOMA-enabled IoT networks', *IEEE Transactions on Vehicular Technology*, vol. 69, no. 12, pp. 15284-15297, https://doi.org/10.1109/TVT.2020.3038387

Kurniawati, AM, Sutisna, N, Zakaria, H, Nagao, Y, Mengko, TL, & Ochi, H 2023, 'High throughput and low latency wireless communication system using bandwidth-efficient transmission for medical Internet of Thing', *International Journal of Technology*, vol. 14, no. 4, pp. 932-947, https://doi.org/10.14716/IJTECH.V14I4.5234

Li, S, Jia, T, Yang, H, Gao, R, & Yang, Q 2023, 'SWIPT cooperative protocol for improving the communication quality of cell-edge users in NOMA network and its performance analysis', *Electronics*, vol. 12, no. 17, article 3583, https://doi.org/10.3390/ELECTRONICS12173583

Liu, Y, Mousavifar, SA, Deng, Y, Leung, C, & Elkashlan, M 2016, 'Wireless energy harvesting in a cognitive relay network', IEEE Transactions on Wireless Communications, vol. 15, no. 4, pp. 2498-2508, https://doi.org/10.1109/TWC.2015.2504520

Mukherjee, S, Kim, D, & Lee, J 2021, 'Base station coordination scheme for multi-tier ultra-dense networks', *IEEE Transactions on Wireless Communications*, vol. 20, no. 11, pp. 7317-7332, https://doi.org/10.1109/TWC.2021.3082625

Nasir, AA, Zhou, X, Durrani, S, & Kennedy, RA 2013, 'Relaying protocols for wireless energy harvesting and information processing', *IEEE Transactions on Wireless Communications*, vol. 12, no. 7, pp. 3622-3636, https://doi.org/10.1109/TWC.2013.062413.122042

Park, J, Lee, N, & Heath, RW 2016, 'Cooperative base station coloring for pair-wise multi-cell coordination', IEEE Transactions on Communications, vol. 64, no. 1, pp. 402-415, https://doi.org/10.1109/TCOMM.2015.2495355

Popovski, P, Fouladgar, AM, & Simeone, O 2012, 'Interactive joint transfer of energy and information', *IEEE Transactions on Communications*, vol. 61, no. 5, pp. 2086-2097, https://doi.org/10.1109/TCOMM.2013.031213.120723

Priyadarshi, R, & Gupta, B 2020, 'Coverage area enhancement in wireless sensor network', *Microsystem Technologies*, vol. 26, no. 5, pp. 1417-1426, https://doi.org/10.1007/S00542-019-04674-Y

Ramly, AM, Amphawan, A, Xuan, TJ, & Kian, NT 2023, 'Analysis of OAM modes and OFDM modulation for outdoor conditions', *International Journal of Technology*, vol. 14, no. 6, pp. 1266-1276, https://doi.org/10.14716/IJTECH.V14I6.6637

Sedtheetorn, P, & Chulajata, T 2016, 'Spectral efficiency evaluation for non-orthogonal multiple access in Rayleigh fading', *In:* International Conference on Advanced Communication Technology (ICACT), 2016-March, pp. 747-750, https://doi.org/10.1109/ICACT.2016.7423544

Shin, W, Vaezi, M, Lee, B, Love, DJ, Lee, J, & Vincent Poor, H 2017., 'Non-orthogonal multiple access in multi-cell networks: theory, performance, and practical challenges', *IEEE Communications Magazine,* vol. 55, no. 10, pp. 176-183, https://doi.org/10.1109/MCOM.2017.1601065

Su, X, Yu, HF, Kim, W, Choi, C, & Choi, D 2016a, 'Interference cancellation for non-orthogonal multiple access used in future wireless mobile networks', Eurasip Journal on Wireless Communications and Networking, vol. 2016, no. 1, pp. 1-12, https://doi.org/10.1186/S13638-016-0732-Z

Su, X, Yu, HF, Kim, W, Choi, C, & Choi, D 2016b, 'Interference cancellation for non-orthogonal multiple access used in future wireless mobile networks', Eurasip Journal on Wireless Communications and Networking, vol. 2016, no. 1, pp. 1-12, https://doi.org/10.1186/S13638-016-0732-Z

Sun, SY, Chen, HH, & Meng, WX 2015, 'A survey on complementary-coded MIMO CDMA wireless communications', *IEEE Communications Surveys and Tutorials*, vol. 17, no. 1, pp. 52-69, https://doi.org/10.1109/COMST.2014.2332999

Tseng, HW, Lee, YH, Lin, JY, Lo, CY, & Jan, YG 2012, 'Performance analysis with coordination among base stations for next generation communication system', *Progress In Electromagnetics Research B*, vol. 36, pp. 53-67, https://doi.org/10.2528/PIERB11072008

Zuhra, SU, Perlaza, SM, Poor, HV, & Altman, E 2022, 'Simultaneous information and energy transmission with finite constellations', *In:* IEEE Information Theory Workshop, https://doi.org/10.1109/ITW48936.2021.9611494

Varshney, LR 2008, 'Transporting information and energy simultaneously', *IEEE International Symposium on Information Theory - Proceedings*, pp. 1612-1616, https://doi.org/10.1109/ISIT.2008.4595260

Yang, Z, Ding, Z, Wu, Y, & Fan, P 2017, 'Novel relay selection strategies for cooperative NOMA', *IEEE Transactions on Vehicular Technology*, vol. 66, no. 11, pp. 10114-10123, https://doi.org/10.1109/TVT.2017.2752264

Yetgin, H, Cheung, KTK, El-Hajjar, M, & Hanzo, L 2017, 'A survey of network lifetime maximization techniques in wireless sensor networks', *IEEE Communications Surveys and Tutorials*, vol. 19, no. 2, pp. 828-854, https://doi.org/10.1109/COMST.2017.2650979

Zhou, N, Hu, J, & Hou, J 2021, 'Research on energy efficiency of NOMA-SWIPT cooperative relay network using GS-DinkelBach algorithm', *Sensors*, vol. 21, no. 17, article 5720, https://doi.org/10.3390/S21175720